Notes on HARDI data preprocessing: Effect on CSD fit

Scott Trinkle

Last edited: February 15, 2019

1 Introduction

These notes describe the effect of HARDI data denoising on the resulting fiber orientation distribution function (fODF) calculated using constrained spherical deconvolution (CSD) [1].

fODF fitting was performed using the `csdeconv` module in the `DIPY` python package. The fiber response function was estimated from the data using a recursive algorithm [2], initiated with a high FA mask from the tensor fit. fODFs were then reconstructed up to a maximum spherical harmonic degree $L_{\max} = 8$, based on the recommendations of a 2013 Tournier paper [3], which finds/claims that "$\ell = 8$ is the highest harmonic degree that could potentially have a detectable influence on the DW signal" (Note: this conclusion is based on empirical analysis of *in vivo* human data with 3 mm^3 isotropic resolution and 500 DW directions. We need to think through how this applies to our data.)

fODFs were calculated from the raw data, as well as from the data denoised with sliding windows of $5 \times 5 \times 5$, $7 \times 7 \times 7$, and $9 \times 9 \times 9$. As with the tensor fit comparison, the volumes were not registered before computing the fODFs, in order to isolate the effect of denoising.

2 Comparison metrics

2.1 Fiber response function

The fiber response function is defined to be symmetric about the z-axis, such that its spherical harmonic representation has $c_{\ell m} = 0$ for $m \neq 0$, where $c_{\ell m}$ is the coefficient for the real spherical harmonic function Y_ℓ^m. Figure 1 shows a comparison of the absolute value of these coefficients (a proxy for "power" in each harmonic degree) estimated from the raw and denoised datasets.

In general the estimated response functions are similar. The difference between raw and denoised coefficients increases for higher harmonic degrees.

2.2 fODF scalar metrics

Here we present comparisons of scalar metrics derived from the fODFs of the raw and denoised data. Note that all comparisons were restricted to fODFs located within a brain mask.

2.2.1 GFA

Generalized fractional anisotropy (GFA) is defined as [4]:

$$\text{GFA} = \sqrt{\frac{N \sum_i^N (\Psi_i - \bar{\Psi})^2}{(N-1) \sum_i^N \Psi_i^2}}, \tag{1}$$

where Ψ is the fODF sampled discretely at N points on the unit sphere, and the overbar denotes a mean over those sample points. Figure 2 shows the distribution of percent differences in GFA between the raw and denoised fODFS, calculated
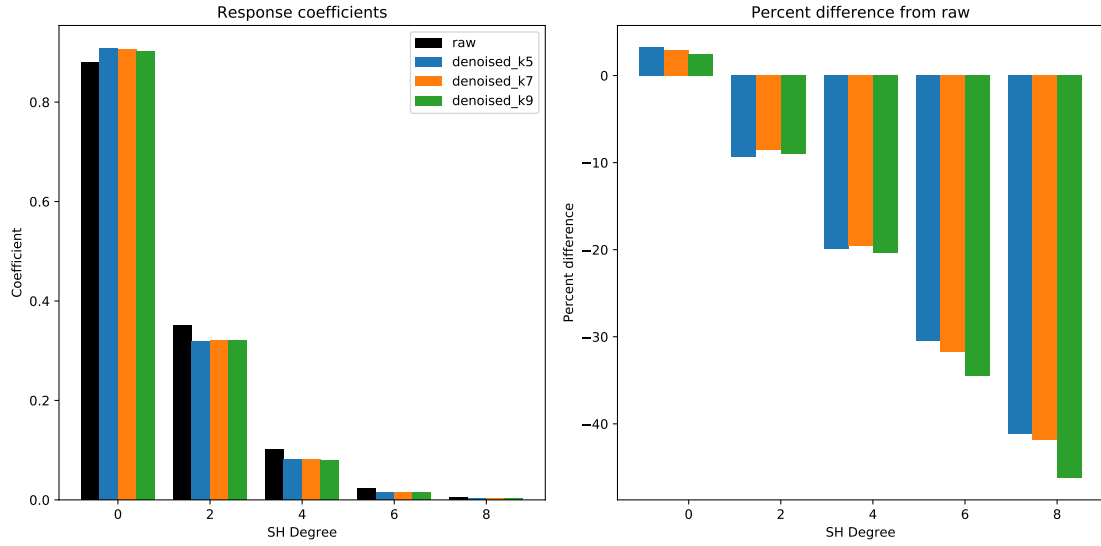
Figure 1: Left) SH representation of the fiber response functions. Right) percent difference between fiber response functions estimated from raw and denoised datasets of various window sizes.

as:

$$\text{Percent Difference} = \frac{\text{GFA}_{\text{denoised}} - \text{GFA}_{\text{raw}}}{\text{GFA}_{\text{raw}}} * 100. \tag{2}$$

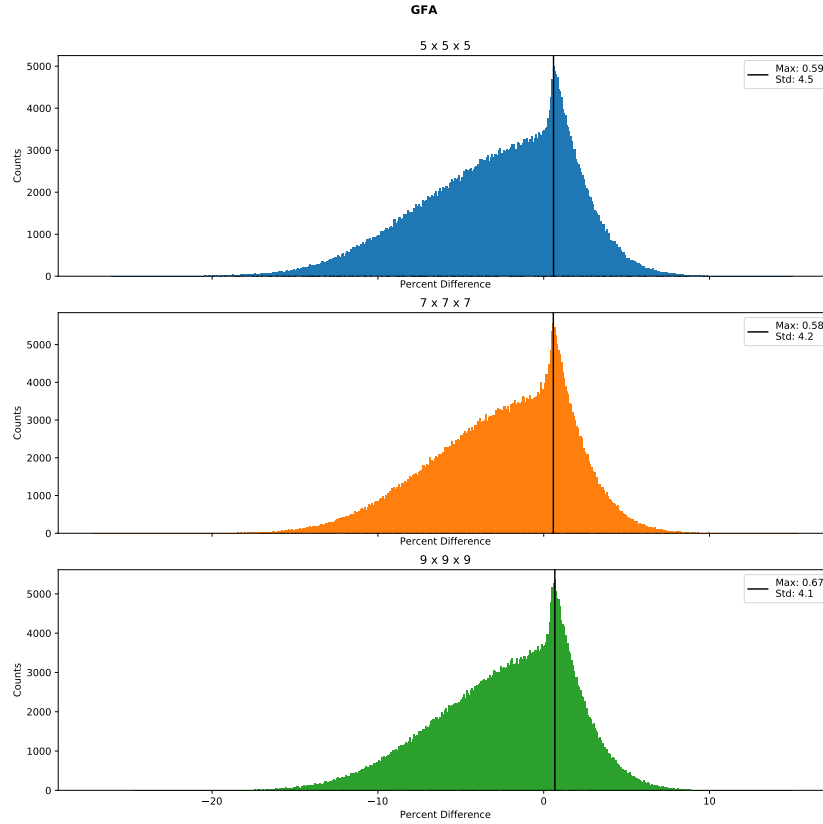(Note that all calculations of percent difference in these notes use the same form presented above.)

Figure 2: Distributions of percent difference in GFA between raw and denoised fODFs.

We see that the distributions peak with a difference around 0.6%, but skew negative, indicating that the denoised fODFs tend to have a smaller GFA than the raw fODFs. This agrees with the results from the response function comparison: the denoised fODFs and response function are more isotropic and have less power at high angular frequency bands than the raw fODFs. This makes intuitive sense: any high frequency noise in the raw data carries over into high angular frequency noise in the reconstructed fODF.

2.2.2 Number of peaks

Peaks in the fODFs are defined as points on the fODF that are greater than at least one neighbor and greater than or equal to all neighbors (a perfectly isotropic fODF would thus have zero peaks). In this study, peaks were also filtered by their relative size (only including peaks with height greater than 0.5 of the greatest peak height) and spacing on the sphere (only including peaks with an angular separation greater than 25 degrees of any larger peaks). Up to five peaks were saved at each voxel.

Figure 3 shows the distribution of the difference in the number of peaks between the raw and denoised data. For all sliding window widths, the distributions are symmetric about zero.
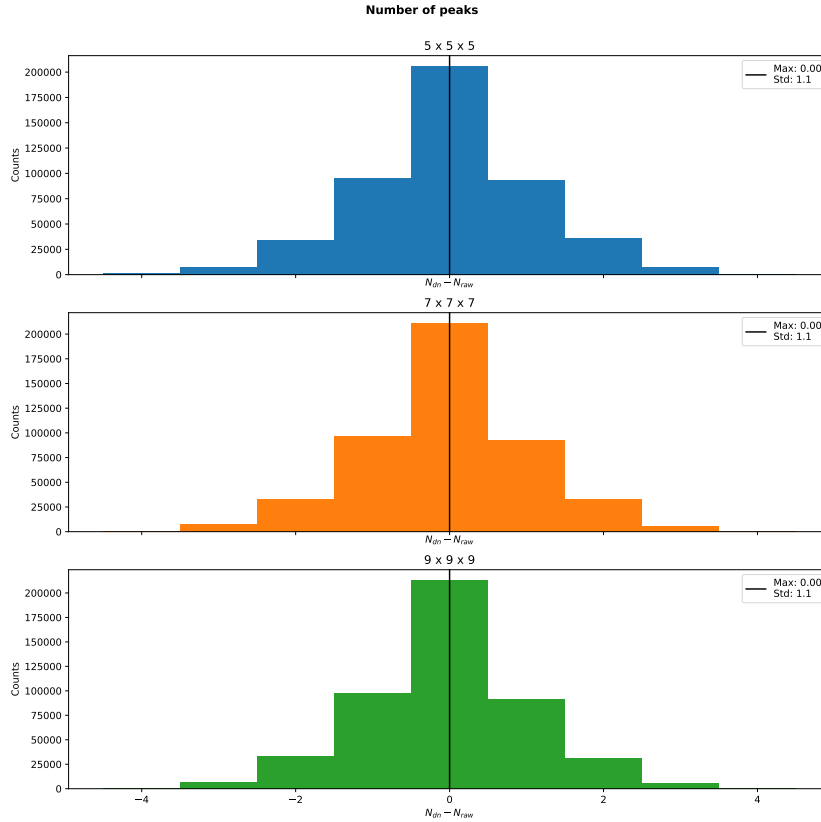

Figure 3: Distributions of difference in number of peaks between raw and denoised fODFs.

2.2.3 Angular separation

Masks were created to only select voxels in which the fODFs for all raw and denoised volumes had exactly two peaks. Figure 4 shows the distribution of angular separations between these peaks in the denoised and raw volumes. The large gap between the $0°$ bin and the rest of the distribution is due to the discretization of the sphere. The peak-finding algorithm used 724 sampling points spaced roughly uniformly across the sphere, with a mean angular separation distance between neighboring sample points of $7°$ degrees. Accordingly, if the peak-finding algorithm does not place the peak at the exact same sample point in both fODFs, in most cases it cannot be placed closer than $7°$.
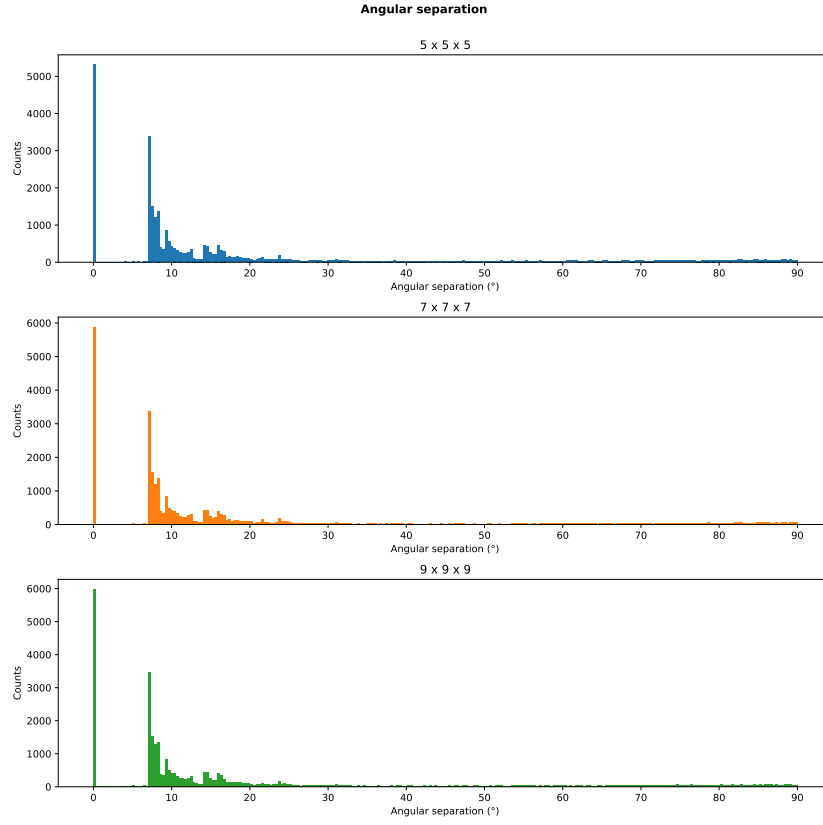
Figure 4: Distributions of angular separation between peaks in the raw and denoised fODFs (for fODFs with two peaks).

2.2.4 Angular Frequency Power

Finally, I looked at the distributions of the percent difference in power in each spherical harmonic degree, defined as:

$$P_\ell = \sum_{m=-\ell}^{\ell} c_{\ell m}^2 \tag{3}$$

Figure 5 shows these distributions as boxplots at each harmonic degree. Generally, the denoised fODFs have more power in the $\ell = 2$ band, and less or equal power for other bands. Additionally, the variance of the percent difference in power tends to get larger at higher harmonic degrees Figure 6 shows the same information while only considering fODFs with GFA >= 0.85. Generally, the percent differences are closer to zero, with lower variance, suggesting that sharper, more unidirectional fODFs are less sensitive to denoising.
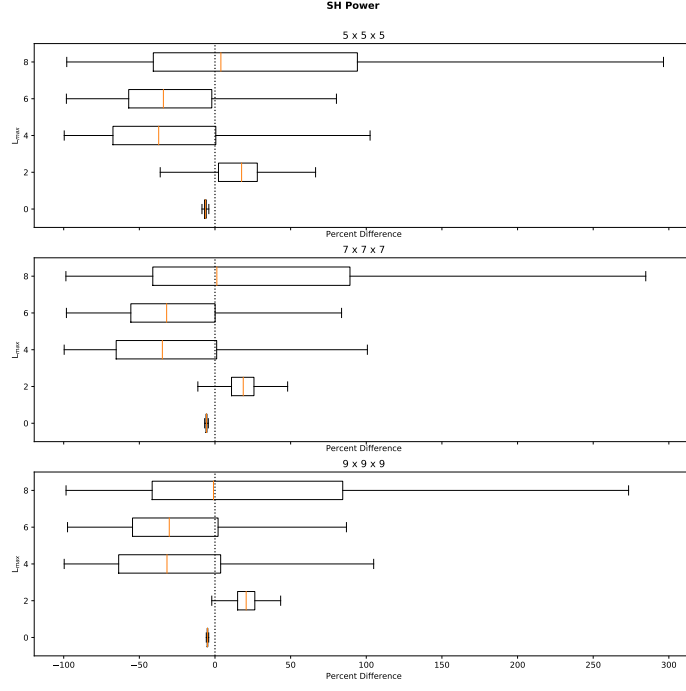
4

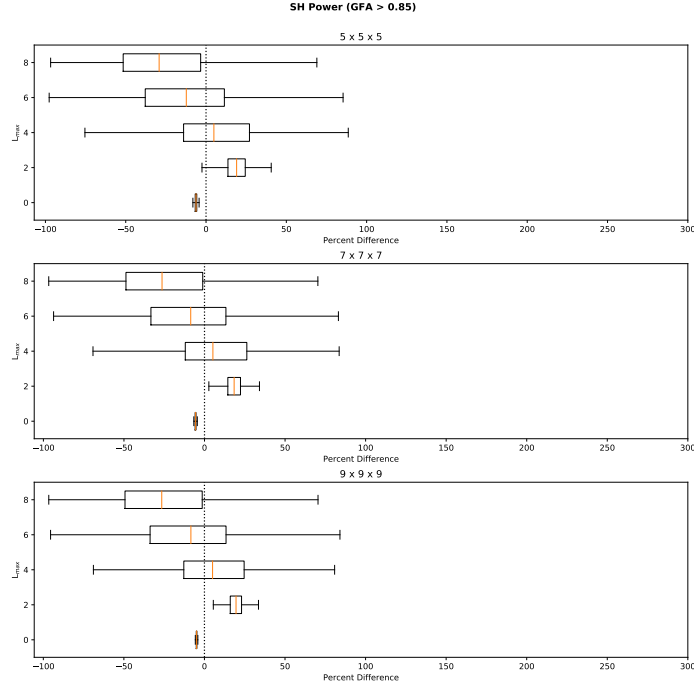Figure 5: Distributions of percent differences in power for each SH degree.

Figure 6: Distributions of percent differences in power for each SH degree. fODFs are restricted to only include those with GFA >= 0.85

3 Conclusion

Similarly to the results from the tensor fit, the overall conclusion from these comparisons is that denoising has some effect on various metrics calculated from the fODFs, and this effect is not dramatically sensitive to the choice of sliding window size in the denoising algorithm. Again, without ground truth fODFs for comparison, we cannot conclude much else about

the value of denoising or the optimal sliding window size.

The next step for this project is to acquire the microCT data and begin working through registration challenges that will arise if we end up needing to section the sample. If we do section the sample: we now have a full CSD reconstruction of the dataset — I can look into doing tractography across the whole brain to identify potentially important tracts we should avoid.

References

[1] J.-D. Tournier, F. Calamante, and A. Connelly, "Robust determination of the fibre orientation distribution in diffusion MRI: Non-negativity constrained super-resolved spherical deconvolution," *NeuroImage*, vol. 35, pp. 1459–1472, may 2007.

[2] C. M. Tax, B. Jeurissen, S. B. Vos, M. A. Viergever, and A. Leemans, "Recursive calibration of the fiber response function for spherical deconvolution of diffusion MRI data," *NeuroImage*, vol. 86, pp. 67–80, feb 2014.

[3] J.-D. Tournier, F. Calamante, and A. Connelly, "Determination of the appropriate b-value and number of gradient directions for high-angular-resolution diffusion-weighted imaging," *NMR in Biomedicine*, vol. 26, pp. 1775–1786, dec 2013.

[4] J. Cohen-Adad, M. Descoteaux, and L. L. Wald, "Quality assessment of high angular resolution diffusion imaging data using bootstrap on Q-ball reconstruction," *Journal of Magnetic Resonance Imaging*, vol. 33, pp. 1194–1208, may 2011.